



1 **On the role of the South Pacific subtropical high**
2 **at the onset of El Niño events**

3
4 Youjia ZOU¹, Xiangying XI^{2*}

5
6 ¹Department of Meteorology and Oceanography, Shanghai Maritime University, Shanghai 201306, China.

7 ²Wuhan University of Technology, 122 Luoshi Road, Wuhan 430070, China.

8
9 Youjia ZOU: marscar@126.com

10 *Xiangying XI: xxy9898@aliyun.com

11 *Correspondence to: xxy9898@aliyun.com

12

13 **Abstract**

14 **Previous studies have suggested that an eastward propagation of the warm pool**
15 **in the western Pacific during El Niño events may be induced by a weakening of**
16 **the easterly Trade Winds (Alexander et al. 2002; Bjerknes 1969). However, the**
17 **dynamic mechanism of the Trade Winds weakening is not well understood. Here**
18 **we use a model and other published proxy records to demonstrate that the**
19 **anomalous southward shift of the south Pacific subtropical high (SPSH) may**
20 **play a crucial role at the onset of El Niño events. By analyzing the relationship**
21 **between the Trade Winds, the Equatorial Currents, the Eastern Boundary**
22 **Currents and the SPSH, we find that an anomalous southward shift of the SPSH**
23 **can result in a weakening of the SE Trade Winds and a southward intrusion of**
24 **the NE Trade Winds, leading to a southward migration of the Trade**
25 **Wind-induced Equatorial Currents, including the Equatorial Countercurrent**
26 **(from ~5°–8°N to ~0°). The warm pool in the western equatorial Pacific is**



27 therefore forced to propagate eastward by the enhanced Equatorial
28 Countercurrent and, thus, a warm phase in the central or the eastern equatorial
29 Pacific. Moreover, the equatorward upwelling in the eastern South Pacific,
30 usually recurving along the equator, shifts southward along with the SPSH, in
31 turn diverts towards the west at $\sim 15^{\circ}\text{S}$ to feed the westward South Equatorial
32 Currents, resulting in a failure of cooling sea surface in the eastern tropical
33 Pacific, thus a flattening of the thermocline. The model experiments indicate that
34 the meridional position and intensity of the Equatorial Countercurrent in the
35 Pacific are some of the determining factors in giving rise to El Niño diversity,
36 suggesting that there should be more frequent warm events due to a meridional
37 expansion of the warm pool under global warming.

38 Key Words

39 El Niño; subtropical high; southward shift; weakening of the trade winds; southward
40 shift of the equatorial currents; southward shift of the upwelling;

41

42

43 Introduction

44 The El Niño phenomenon, characterized by anomalous Trade Winds and sea surface
45 temperatures (SSTs) in the tropical Pacific (Bjerknes 1969; Ramesh & Murtugudde
46 2013), is considered to have global implications with costly consequences. Presently
47 there is a general agreement in the fields of the atmospheric and oceanic science that
48 the warm pool (SSTs greater than about 29°C) in the western Pacific propagating



49 eastward along the equator is induced by the weakening of the Trade Winds
50 (McPhaden 1999). This picture, however, leaves open the question of why and how
51 the Trade Winds weaken. Despite a variety of mechanisms being proposed (Bjerknes
52 1969; Wyrski 1975; Oldenborgh 2000), there is no scientific consensus on how the
53 Trade Winds slacken or even reverse. The apparent absence of a super warm phase in
54 2014 that was expected by many models implies that we may still not understand
55 some fundamental aspects of the system. Over the past decades, investigations into
56 the tropical Pacific's role at the onset of El Niño events mainly focused on the SST
57 anomalies (that is, deviations from climatological norms) (Rasmussen & Carpenter
58 1982), recharge/discharge of equatorial upper-ocean heat content (Meinen &
59 McPhaden 2000) and westerly wind bursts (Lengaigne 2004; Fedorov et al. 2014).
60 Recently, the westward equatorial currents were found to be enhanced during La Niña
61 but distinctly reversed during extreme El Niño events (Santoso et al. 2013). Our
62 investigations show that all the above are likely to be directly associated with the
63 South Pacific Subtropical High system (hereafter referred to as SPSH), which has
64 potential (because the Trade Winds, the Westerlies and the Eastern Boundary
65 Currents are all mainly associated with the SPSH and further develop with it in
66 position and intensity) to dominate climate change in South Pacific region by creating
67 significant impacts on the Trade Winds, precipitation patterns and ocean circulations
68 (**Figs.1a-b**). We therefore hypothesize that there may be a critical role played by the
69 SPSH at the onset of El Niño events.

70



71 Each year, the South Pacific experiences a seasonal cycle with a northward/southward
72 shift of the subtropical high (SH) in austral winter/summer from $\sim 16^{\circ}\text{S}$ to $\sim 35^{\circ}\text{S}$
73 (Reid et al. 1958). It is generally accepted that the seasonal migrations of the SPSH
74 cannot make significant impacts on the Trade Winds, the Equatorial Currents and the
75 Eastern Boundary Currents due to its nonlinear mechanism. Nevertheless, above
76 seasonal migrations may be disturbed when the South Pacific undergoes a
77 perturbation from external forcings, for example, an insolation weakening, leading to
78 an anomalous displacement of the SPSH (**Figs.1a-b**). Evidence shows that the SH is
79 sensitive to the external forcings (Reid et al. 1958).

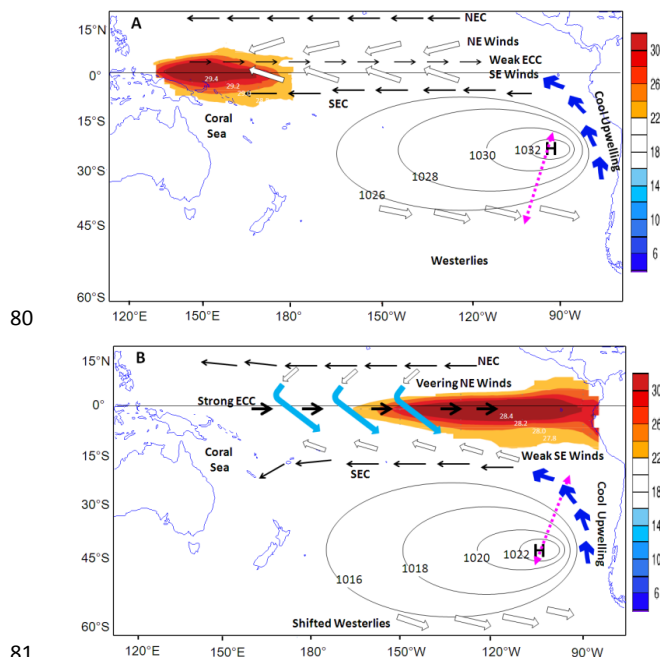


Fig 1. Comparison between normal and El Niño conditions. A, normal condition with strong trade winds, weak ECC and intense upwelling recurving along the equator. Warm waters brought by the weak ECC mix with the strong upwelling in the central equatorial Pacific. **B**, El Niño condition with a southward shifted SPSH (along with the SE trade winds, equatorial currents and westerlies), veered NE trade winds, strong ECC and weak upwelling deflecting to the west at $\sim 15^{\circ}\text{S}$. Warmer waters brought by the strong ECC mix with the weak upwelling in the eastern South Pacific, leading to SSTs



88 anomalies. The dashed arrows in pink color denote the approximate trajectory of the SPSH shift. The
89 solid light blue arrows denote veering Trade Winds. The hollow arrows, solid black arrows and solid
90 dark blue arrows represent the climatological winds, currents and cool upwelling, respectively. The
91 Trade Winds are symmetric about the wind equator (about $\sim 5^{\circ}\text{N}$ - 8°N) in normal condition, rather than
92 the geographic equator.

93

94 An anomalous southward migration of the SPSH can result in a weakening of the SE
95 Trade Winds and an enhancement of the Equatorial Countercurrent (ECC),
96 concurrently allowing for a southward incursion of the NE Trade Winds (**Fig.1b**). As
97 the Trade Wind system shifts southerly, so do the Trade Wind-induced equatorial
98 currents. The Pacific ECC (hereafter referred to as ECC), the strongest (more than 20
99 Sv) compared with its counterparts (Yu et al. 2000), residing between the North
100 Equatorial Current (NEC) and the South Equatorial Current (SEC), with its mean axis
101 usually around 5°N in winter and 8°N in summer (Yu et al. 2000; Tomczak &
102 Godfrey 2003), migrates to about 0° or more south in response to the southward shifts
103 of the Trade Wind system, advecting the giant pool of the warm waters eastward
104 along the equator (**Fig.1b**). In essence, Wyrtki postulated in 1973 that an unusually
105 strong ECC in the western Pacific would lead to an anomalous accumulation of the
106 warm water in the eastern equatorial Pacific and, thus, El Niño event (Wyrtki 1973),
107 but his suggestion has long been overlooked due to lack of plausible mechanisms and
108 a failure of explaining why the warm pool propagates along the equator rather than
109 along the $\sim 5^{\circ}\text{N}$ or $\sim 8^{\circ}\text{N}$ of latitude.

110

111 In addition, a southward migration of the NE Trade Winds can result in a veering of
112 the NE Trade Winds from northeast to northwesterly or westerly under the influence



113 of the Coriolis force after the NE Trade Winds cross the equator, further amplifying
114 the intensifying of the ECC (**Fig.1b**). Meanwhile, a relaxation of the SEC in response
115 to a weakening of the easterly winds is liable to lead to less build-up of heat content in
116 the western tropical Pacific but more heat is retained in the central and the eastern
117 tropical Pacific (McPhaden 1999). The net result of all the above is a reversal of the
118 Walker Circulation, creating westerly winds in the western tropical Pacific and
119 intensifying the eastward ECC, thus establishing a positive feedback. It is noteworthy
120 that the source of the ECC has changed from the warm water to warmer water with
121 southward shifts of its main axis from $\sim 5^{\circ}\text{N}$ - 8°N to $\sim 0^{\circ}$, fueling the reversal of the
122 Walker Circulation and the warming in the central and the eastern equatorial Pacific.
123 Moreover, the upwelling in the eastern South Pacific, which usually recedes along
124 the equator, shifts southward along with the Trade Winds/SPSH, in turn diverts
125 towards the west at $\sim 15^{\circ}\text{S}$ during El Niño events to feed the westward SEC
126 (**Figs.1a-b**), resulting in a failure of cooling sea surface in the eastern tropical Pacific,
127 thus a flattening of the thermocline.

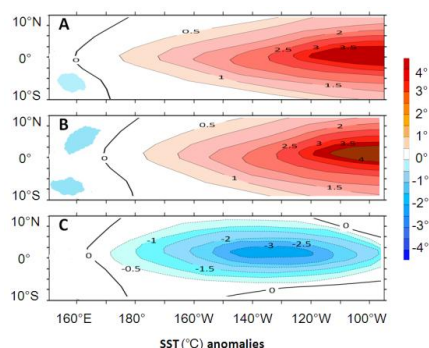
128

129 **Simulating El Niño events**

130 To test whether the SPSH acts as a possible trigger at the onset of El Niño events, we
131 carry out simulation experiments in which we examine the response of SSTs in the
132 tropical Pacific to the observed location and intensity of the SPSH added to a
133 comprehensive climate GCM, HadOPA, which couples the OPA (ocean model) and
134 HadAM3 (atmospheric model) through OASIS 2.4 (Lengaigne et al. 2004 & 2006).



135 (For details of the model description, see Methods). We slightly modify this model
136 and assume that the surface wind stress anomaly and the ECC anomaly are a function
137 of the position and strength of the SPSH (see Methods). When the surface wind stress
138 and the meridional position of the ECC vary by artificially tuning the position and
139 strength of the SPSH as a perturbation, the interannual oscillations with SST
140 anomalies retain little change at the initial stage due to its nonlinear effects but start to
141 surge and become highly irregular as the SPSH continuously moves southward in
142 early spring with a gradual weakening. When further perturbation is imposed in late
143 spring, the model produces a broad continuum of El Niño events subsequently in
144 position ranging from the dateline to the eastern tropical Pacific (Extended Data
145 **Figs.3a-c**). A strong El Niño event occurs in winter in the eastern tropical Pacific as
146 an intense southward shift of the SPSH superimposed on the seasonal cycle takes
147 place (Extended Data **Fig.3c** and Methods). However, a relative weak El Niño event
148 appears in summer around the dateline when a weak southward migration of the
149 SPSH occurs (Extended Data **Fig.3a** and Methods). We run this model by changing
150 the meridional position anomalies of the SPSH ($\Delta\phi_{\text{sph}}$) to $\sim+10^\circ$ and $\sim+12^\circ$ of
151 latitude (observed location anomalies), respectively, with a gradual weakening, to
152 simulate the El Niño episodes in 1982 and 1997. As expected, the warm events
153 quickly develop into extreme EP El Niño events with SST anomalies in Niño3
154 exceeding 3.8°C and 4.2°C , respectively, consistent with the observations (**Figs.2a-b**).
155 (data available online at <http://www.cpc.noaa.gov/data/indices>)



156

157 **Fig 2. Simulated El Niño and La Niña.** **A**, a strong El Niño in the eastern tropical Pacific as the $\Delta\phi_{\text{spsh}}$
158 is $\sim +10^\circ$ of latitude. **B**, a stronger El Niño in the eastern tropical Pacific as the $\Delta\phi_{\text{spsh}}$ is $\sim +12^\circ$ of
159 latitude. **C**, a La Niña near the eastern tropical Pacific as the $\Delta\phi_{\text{spsh}}$ is $\sim -4^\circ$ of latitude with zonal
160 position anomalies ($\Delta\lambda_{\text{spsh}}$) $\sim +7^\circ$ of longitude (an eastward anomaly is positive).

161

162 **Simulating La Niña**

163 Similar model experiments have been done to simulate the La Niña episode in 2008

164 by moving the SPSH northerly. The simulation experiments indicate that the warm

165 phase in the eastern tropical Pacific subsequently evolves into a cold phase in late

166 summer the next year as the $\Delta\phi_{\text{spsh}}$ is about $\sim -4^\circ$ of latitude (a northward anomaly is

167 negative) and the zonal position anomalies ($\Delta\lambda_{\text{spsh}}$) are $+7^\circ$ of longitude (an eastward

168 anomaly is positive), with 2°C – 3°C cooling of SST anomalies in Niño3 region

169 (**Fig.2c**), reasonably consistent with the observed records. Northward shifts of the

170 SPSH can enhance the SE Trade Winds and the SEC, weaken the ECC and push the

171 SEC and ECC northwards, leading to a westward shift of the warm pool and the

172 atmospheric convection in the equatorial Pacific. Whether an El Niño event is

173 followed by a La Niña principally rests with the $\Delta\phi_{\text{spsh}}$ and the upwelling feedbacks

174 which are mainly determined by the southerly onshore winds in the eastern part of the

175 SPSH (Rollenbeck et al. 2015). The upwelling feedbacks tend to be stronger when the



176 zonal pressure gradients in the eastern part of the SPSH are steeper (more dense
177 isolines) and the center position of the SPSH from South American coast is more
178 favorable (**Fig.6c**). The simulation experiments suggest that an approximately
179 NNE-SSW oriented trajectory of the SPSH shift is conducive to more steep zonal
180 pressure gradients in the eastern part of the SPSH when the SPSH shifts northerly
181 according to the theory of fluid mechanics and Bernoulli's theorem, generating more
182 intense upwelling (the shifting trajectory of the SPSH centre and coast line produce a
183 duct-like passage for the southerly onshore winds with a narrow opening in the north
184 and a relatively wide opening in the south) (**Fig.1b**). In addition, a more northerly
185 location of the SPSH tends to bring the upwelling to the right position (around equator)
186 in the eastern equatorial Pacific, favoring a La Niña. However, in realistic regimes,
187 the transit from a warm phase to a cold phase may be slightly different from that
188 created by our theoretical models, possibly involving a more complex process, such as
189 an oscillating, a pause or a prolonged evolution, etc.

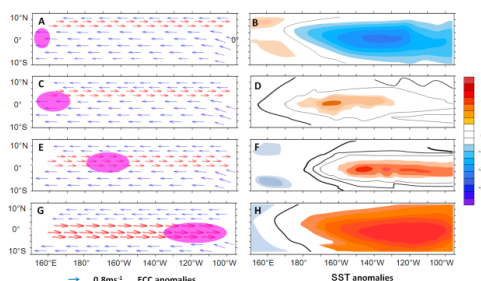
190

191 **Simulating ECC anomalies**

192 The experiment in simulating the response of the meridional position anomalies of the
193 ECC ($\Delta\phi_{ecc}$) to the $\Delta\phi_{sps}$ indicates that the $\Delta\phi_{ecc}$ nonlinearly corresponds to the $\Delta\phi_{sps}$
194 (**Figs.3a-d, extended data Fig.5**), suggesting that the meridional position and
195 intensity of the ECC are some of the determining factors in giving rise to El Niño
196 diversity. A strong ECC in an appropriate meridional position (around the equator)
197 tends to advect more warm waters to the eastern equatorial Pacific and produce an



198 extreme EP El Niño (a more southerly position of the ECC in winter is easier to be
199 pulled down to the equator, offering a sufficient explanation for extreme El Niño
200 events always occurring in winter) (**Fig.3d**), implying that there should be more
201 frequent warm events due to a meridional expansion of the warm pool in the western
202 equatorial Pacific and an acceleration of the Hadley Cell (poleward shifts of the
203 descending points) under global warming (Cravatte et al. 2009).



204

205 **Fig 3. Simulated ECC anomalies and corresponding SST anomalies.** **A** and **B**, a weak ECC in La
206 Nina condition and corresponding SST anomalies. **C** and **D**, a moderate and southward shifted ECC as
207 the $\Delta\phi_{\text{sps}}h$ is $\sim +7^\circ$ of latitude and corresponding SST anomalies. **E** and **F**, a strong, broad and
208 southward shifted ECC as the $\Delta\phi_{\text{sps}}h$ is $\sim +10^\circ$ of latitude and corresponding SST anomalies. **G** and **H**,
209 a stronger, broader and southward shifted ECC as the $\Delta\phi_{\text{sps}}h$ is $\sim +11^\circ$ of latitude and corresponding
210 SST anomalies. The warm pool is brought to the central or eastern equatorial Pacific by the southward
211 shifted ECC. The red and blue arrows represent the ECC and the NEC/SEC, respectively. The shading
212 area denotes the warm pool on the left panels.

213

214 Discussion

215 A key question being debated for long time is whether the southward migration of the
216 SPSH is a passive response to El Niño events or is a driver to El Niños. Traditionally,
217 the southward migrations of the SPSH are thought by some authors to be a result of El
218 Niños (McPhaden, 1999; Meinen & McPhaden 2000; Oldenborgh 2000). In contrast,
219 our investigation reveals that a southward shift of the SPSH is not a passive response
220 to El Niño events but is driving El Niño events. This reasoning is based on the



221 asymmetric response of the North Pacific Subtropical High (NPSH) and the SPSH to
222 the eastward SSTs anomalies (the equatorward displacements of the NPSH were
223 observed in winter during El Niño events), inconsistent with that both the NPSH and
224 SPSH should be synchronously affected by the eastward SSTs anomalies if the
225 southward migration of the SPSH were the result of El Niño events. Besides, the
226 SPSH is a large-scale permanent pressure system produced by the global general
227 circulation of the atmosphere, rather than by an individual equatorial low pressure belt
228 in the equatorial Pacific. Therefore the SPSH is not likely to be driven by a regional
229 system, such as the local warming/cooling in the equatorial Pacific. Furthermore, the
230 anomalous migrations of the SH have also been identified in other oceans (Zou et al.
231 2017).

232

233 The strong support for the southward shifts of the SPSH not being forced by the
234 eastward warm pool during El Niño events comes from two independent
235 investigations into proxy records and experiments throughout the Holocene. The
236 fluctuations of the iron concentrations, which are thought to reflect the precipitation
237 patterns in southern Chile, intimately linking with the westerlies (Lamy et al. 2001),
238 are qualitatively consistent with the periods of ENSO (Moy et al. 2002) in the past 8
239 kyr (**Extended Data Fig.4**), suggesting southward displacements of the westerlies in
240 the South Pacific during El Niño events, thus implying the concurrent shifts of the
241 SPSH (because the westerlies are mainly associated with the SPSH and further
242 develop with it in position and intensity). The solar sensitivity experiments with a



243 comprehensive global climate model indicate that the southward migrations of the
244 westerlies are in line with the variations of solar forcing (Varma et al. 2001), implying
245 that the southward shifts of the SPSH during El Niño events are likely attributed to
246 solar activity, rather than El Niño itself, and further supporting our hypothesis.
247 Furthermore, the timing of the southward displacements of the westerlies was
248 concurrent with that of the strengthening of the ECC, also suggesting a role of the
249 southward displacements of the SPSH at the onset of El Niño events.

250

251 Another theory worth noting is the “westerly wind burst” which is recently suggested
252 to be a possible trigger of El Niño events (Lengaigne et al. 2004; Fedorov et al. 2014;
253 Menkes et al. 2014). These westerly winds are thought to be a manifestation of the
254 Madden-Julian Oscillation (MJO) which originates over the Indian Ocean, with a 30
255 to 60-day period (Madden & Julian 1972). However, McPhaden (1999) argued that
256 the episodic westerly wind forcing is not a necessary condition for the development of
257 El Niño events because such forcing can be seen during non-El Niño years, and many
258 coupled ocean-atmosphere models also simulate ENSO-like variability without it
259 (McPhaden & Yu 1999). Our investigation shows that the observed “westerly winds”
260 are to some extent ascribed to the veered NE Trade Winds after crossing the equator
261 (subsequently becoming northwesterly or westerly winds), constituting the lower limb
262 of the reversed Walker Circulation in the western-central tropical Pacific during El
263 Niño events. In essence, the Trade Winds in the equatorial Pacific, in contrast to that
264 in the equatorial Atlantic, are not symmetric about the geographic equator, but about



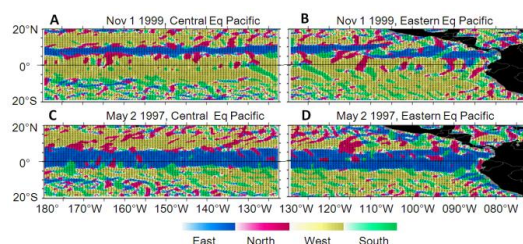
265 the $\sim 5^{\circ}\text{N}$ – $\sim 8^{\circ}\text{N}$ of latitude (climatological mean position, a.k.a. “wind equator”). This
266 region (0° – $\sim 5^{\circ}\text{N}$ in the middle of the Pacific) is actually dominated by the SE Trade
267 Winds with frequency of 40%–50% (Sailing Directions, 2013) rather than by the NE
268 Trade Winds intuitively thought. This is confirmed by Routeing Chart 5127 (UK
269 hydrographic office, 2012), suggesting that the NE Trade Winds start to deflect to
270 northwesterly or westerly (mean extending latitudinally from $\sim 5^{\circ}\text{N}$ to $\sim 10^{\circ}\text{S}$) once
271 beyond the “wind equator”. This explains why the westerly winds can be seen in
272 north of the geographic equator. Occasionally the maximum northern boundary of the
273 westerly winds can reach $\sim 10^{\circ}\text{N}$ under the influence of effects of the entrainment. The
274 ellipse-shaped structure of the SPSH may account for the westerly winds occurring in
275 the western equatorial Pacific first (gradually towards the central Pacific) as the SPSH
276 migrates southward, consistent with the satellite observations indicating reversed
277 Trade Winds mainly confined in the western and central Pacific during El Niño events
278 **(Extended Data Fig.6)**. The model experiments indicate that although the
279 MJO-related westerly wind forcing is not a sufficient condition for the El Niño onset,
280 it can amplify the veered NE Trade Winds if it occurs on time, reinforcing the
281 reversed Walker Circulation and the ECC and, thus, promoting the El Niño-like states
282 to evolve to El Niño events **(Fig.3d)**. This explains why every warm event during the
283 past 50 years was always preceded by the westerly winds (Eisenman et al. 2005).
284
285 The superposition of the MJO-related westerly winds onto the veered NE Trade
286 Winds may contribute to surface water convergence (Chen et al. 2015), promote



287 eastward downwelling equatorial Kelvin waves that create warming phase in the
288 eastern tropical Pacific (McPhaden & Yu 1999), advect the warm pool eastwards and
289 push the ECC southwards and eastwards (Picaut et al. 1997), leading to a broader and
290 stronger ECC (**Figs.3b-d**), consistent with the satellite observations (**Fig.4a-d**). In
291 contrast to some previous studies (Lengaigne et al. 2004; Fedorov et al. 2014), we
292 argue that the eastward propagation of the warm pool in the western equatorial Pacific
293 is likely to be forced mainly by the enhanced and southward shifted ECC rather than
294 by the episodic westerly winds because those westerly winds were observed to be
295 sporadic and not strong enough (Beaufort Scale 5 or less) even if in the most
296 pronounced event in 1997 according to the satellite observations (**Extended Data**
297 **Fig.6**), but these winds may help the eastward development of the warm pool. The
298 likelihood of the westward equatorial currents (SEC) being totally reversed by the
299 sporadic and weak westerly winds is considered low. The newly-discovered “reversed
300 Equatorial Currents” during extreme El Niño events by Santoso et al. (2013), is most
301 likely to be the southward shifted ECC when combined with other evidence from
302 Wyrski (1973), Lamy et al.(2001) and Varma et al.(2011). This is also confirmed by
303 the satellite observations with an absence of the ECC in previous latitudes ($\sim 5^{\circ}\text{N}$ - 8°N)
304 and an emergence of a new eastward equatorial current around the equator during El
305 Niño events (**Fig.4a-d**). The fact that the westward transport of the SEC entering the
306 Coral Sea (in northeast of Australia, **Fig.1a-b**) increases during El Niño events and
307 decreases during La Niña (Kessler & Cravatte 2013) is suggestive of the meridional
308 shifts of the SEC (the climatologically strongest SEC meridionally ranging from $\sim 2^{\circ}\text{N}$



309 to $\sim 6^{\circ}\text{S}$, then gradually weakening towards the south (Yu et al. 2000; Tomczak &
310 Godfrey 2003). Also see Routeing Chart 5127 published by UK Hydrographic Office
311 in 2012), further confirming our speculation.



312
313 **Fig 4. Surface Current derived from satellite observations.** A and B, the positions and directions of
314 the surface currents in the central and eastern equatorial Pacific, respectively, during normal condition
315 (Nov 1, 1999). C and D, the positions and directions of the surface currents in the central and eastern
316 equatorial Pacific, respectively, during El Niño condition (Nov 1, 1997). A broader and southward
317 shifted ECC can be seen around the equator. Different colors denote different directions of the surface
318 currents. <http://www.oceanmotion.org/html/resources/oscar.htm>.

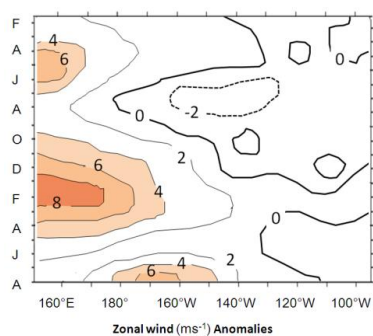
319

320 **Simulating the tropical wind anomalies and upwelling**

321 To further examine the response of the tropical wind anomalies to the position
322 anomalies of the SPSH, we run the model by altering the meridional position of the
323 SPSH alone (Methods). Over the tropical Pacific, the model simulation shows that the
324 tropical wind anomalies closely track the variations of the SPSH. As anticipated, the
325 tropical wind anomalies are not evident by changing the zonal position of the SPSH
326 alone (**Fig.5**). In 1997, the center of the SPSH was observed to shift from 27°S in
327 May to 36°S in August, to 45°S in November, all at about 77°W - 80°W , with zonal
328 wind anomalies at lat 0° long 150°E from 1ms^{-1} in May to 5ms^{-1} in August, to 7.5ms^{-1}
329 in November, respectively (McPhaden 1999). The superposition of the El
330 Niño-related southward shifts of the SPSH onto the seasonal cycle makes the average



331 speed of the SPSH moving nearly 50 percent faster than usual, serving as an
332 alternative precursor for the initial development of the event. This offers the scientists
333 new insights into monitoring and prediction of the El Niño onset.

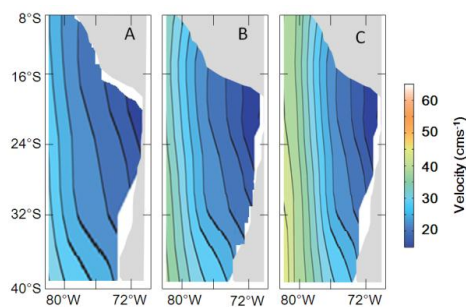


334 **Fig 5.** The response of the zonal wind anomalies in the equatorial tropical Pacific to the
335 meridional position anomalies of the SPSH. The zonal wind anomalies (between 5°N and 5°S) as the
336 $\Delta\varphi_{\text{spsh}}$ is $\sim+7^\circ$ of latitude during Mar-Jun and the zonal wind anomalies as the $\Delta\varphi_{\text{spsh}}$ is $\sim+10^\circ$ of
337 latitude during Nov-Apr.
338

339
340 Similar model experiment has been executed for validating the response of the
341 upwelling to the position anomalies of the SPSH, indicating that the upwelling
342 sharply follows the alterations of the SPSH in zonal position, with the meridional
343 position playing a negligible role (**Figs.6a-c**). The model simulations suggest that the
344 tropical wind anomalies are affected primarily by the meridional position of the SPSH
345 through varying the surface wind stress while the intensity of the upwelling is mainly
346 influenced by the zonal location of the SPSH, with the meridional position and the
347 strength of the SPSH playing a secondary role, consistent with the previous study on
348 the NPSH (Cheshire & Thurow 2013). The zonal pressure gradients near the center of
349 the SPSH are small but it can be huge with strong southerly onshore winds in the
350 eastern part of the SPSH (the densest isolines, **Figs.6b-c**), generating intense



351 upwelling along South American coast if a right zonal position of the SPSH is set.



352

353 **Fig 6.** The response of the upwelling feedbacks to the zonal position anomalies of the SPSH. **A**, the
354 upwelling feedbacks (surface velocity) in normal condition. **B**, the upwelling feedbacks as the $\Delta\lambda_{\text{spsh}}$ is
355 $+6^\circ$ of longitude, **C**, the upwelling feedbacks as the $\Delta\lambda_{\text{spsh}}$ is $+8^\circ$ of longitude (the meridional position
356 and the intensity of the SPSH remain unchanged). The smaller the spacing, the stronger the upwelling
357 feedbacks.

358

359 Conclusion

360 The model experiments suggest that the SPSH may play a critical role at the onset of
361 El Niño events. Further development of El Niño events (diversity) is likely to be
362 influenced by the subsequent air-sea interactions and the interplay between the
363 eastward warm pool in the western tropical Pacific and the unstable mixing state of
364 warm and cold waters in the central or the eastern tropical Pacific. This does not,
365 however, disparage other drivers which may also play a role at El Niño onset.
366 Understanding the role of the SPSH at the onset of El Niño events is important not
367 only because it is capable of fully reconciling the divergent views of El Niño's origin
368 but also because it exhibits a more plausible explanation of El Niño/La Niña. The
369 apparent lack of real-time forecasting and long-term predictability of El Niño at the
370 current stage implies that we have some way to go in fully understanding the real
371 physical mechanisms of the El Niño/La Niña phenomenon. It is believed that our new



372 findings can better shed light on the role of the SPSH in the genesis of El Niño and
373 may lead to more accurate predictions for a longer period in the future.

374

375 **Acknowledgements** authors sincerely acknowledge Trenberth K.E., who is currently
376 working in NCAR, USA, for providing valuable suggestions in the contributors of El
377 Niño onset.

378

379 **Author Contributions** Both authors contributed equally to this work.

380 Zou collected all data, prepared the manuscript and figures, and performed the
381 analysis. Xi was responsible for data collection, laboratory efforts and contributed to
382 the computer programming and the model simulating. Both authors discussed the
383 results and provided inputs to the paper.

384

385

386 **References**

387 Alexander, M. A. et al., 2002: The atmospheric bridge: The influence of ENSO
388 teleconnections on air-sea interaction over the global oceans. *J. Clim.* **15**,
389 2205-2228.

390 Bjerknes, J.A, 1969: Atmospheric teleconnections from the equatorial pacific. *Mon.*
391 *Wea. Rev.* **97**(3):163-172.

392 Chen, D.K. et al., 2015: Strong influence of westerly wind bursts on El Niño diversity.
393 *Nature Geoscience* **8**(5).



- 394 Cheshire, H. & Thurow, J, 2-13: High-resolution migration history of the Subtropical
395 High/Trade Wind system of the northeastern Pacific during the last ~55000 years:
396 Implications for glacial atmospheric reorganization, *Paleoceanography* **28**,
397 319-333.
- 398 Cravatte, S., Delcroix, T., Zhang, D., Mcphaden, M. & Leloup, J, 2009: Observed
399 freshening and warming of the western pacific warm pool. *Clim. Dynam.* **33**(4),
400 565-589.
- 401 Eisenman, I., Yu, L. & Tziperman, E, 2005: Westerly wind bursts: ENSO's tail rather
402 than the dog. *J. Clim.* **18**, 5224–5238.
- 403 Fedorov, A. V., Hu, S., Lengaigne, M. & Guilyardi, E, 2014: The impact of westerly
404 wind bursts and ocean initial state on the development and diversity of El Niño
405 events. *Clim. Dynam.* **44**, 1381-1401.
- 406 Kessler, W.S. & Cravatte, S, 2013: ENSO and Short-Term Variability of the South
407 Equatorial Current Entering the Coral Sea. *J. Phys. Oceanography*.
408 **43**(5):956-969.
- 409 Lengaigne, M. et al., 2004: Triggering of El Niño by westerly wind events in a
410 coupled general circulation model. *Clim Dyn.* **23**(6):601–620.
- 411 Lamy, F., Hebbeln, D., Röhrl, U. & Wefer, G, 2001: Holocene rainfall variability in
412 southern Chile: a marine record of latitudinal shifts of the Southern Westerlies.
413 *Earth & Planetary Science Letters* **185**(s3–4):369-382.
- 414 Madden, R. A. & Julian, P.R, 1972: Description of global-scale circulation cells in the
415 tropics with a 40–50 day period. *J. Atmos. Sci.* **29**, 1109–1123.



- 416 McPhaden, M. J, 1999: Climate oscillations: Genesis and evolution of the 1997–98 El
417 Niño. *Science* **283**, 950-954.
- 418 McPhaden, M. J. & Yu, X, 1999: Equatorial waves and the 1997–1998 El Niño.
419 *Geophys Res Lett* **26**(19):2961-2964.
- 420 Meinen, C. S. & McPhaden, M. J, 2000: Observations of warm water volume changes
421 in the equatorial Pacific and their relationship to El Niño and La Niña. *J. Clim.* **13**,
422 3551-3559.
- 423 Menkes, C. E. et al., 2014: About the role of Westerly Wind Events in the possible
424 development of an El Niño in 2014. *Geophys. Res. Lett.* **41**, 6476–6483.
- 425 Moy, C. M., Seltzer, G. O., Rodbell, D. T. & Anderson, D. M, 2002: Variability of El
426 Niño/Southern Oscillation activity at millennial timescales during the Holocene
427 epoch. *Nature* **420**(6912):162-165.
- 428 Oldenborgh, G. J. V, 2000: What Caused the Onset of the 1997–98 El Niño? *Mon.*
429 *Wea. Rev.* **128**, 2601-2607.
- 430 Picaut, J., Masia, F. & Penhoat, Y. D, 1997: An advective-reflective conceptual model
431 for the oscillatory nature of the ENSO. *Science* **277**, 663-66.
- 432 Ramesh, N. & Murtugudde, R, 2013: All flavours of El Niño have similar early
433 subsurface origins. *Nature Climate Change* **3**(1):42-46.
- 434 Rasmussen, E. M. & Carpenter, T. H, 1982: Variations in sea surface temperature and
435 surface wind fields associated with the Southern Oscillation/El Niño. *Mon. Weath.*
436 *Rev.* **110**, 354-384.
- 437 Reid, J. L., Roden, G. I. & Wyllie, J. G, 1958: Studies of the California Current system,



- 438 Californian Co-operative Oceanic Fisheries Investigations Report. 6, pp. 28–56,
439 La Jolla, Calif.
- 440 Rollenbeck, R. et al., 2015: Climatic Cycles and Gradients of the El Niño Core
441 Region in North Peru. *Advances in Meteorology* **2015**:1-10.
- 442 Santoso, A. et al., 2013: Late-twentieth-century emergence of the El Niño propagation
443 asymmetry and future projections. *Nature* **504**(7478):126-130.
- 444 Tomczak, M. & Godfrey, J. S, 2003: Regional Oceanography: An Introduction, 2nd
445 edition, pp. 390.
- 446 UK Hydrographic Office. Sailing Directions, NP61 & 62, 13th edition, pp 32-39,
447 Taunton , UK (2013).
- 448 Varma, V., Prange, M., Lamy, F., Merkel, U. & Schulz, M, 2011: Solar-forced shifts
449 of the southern hemisphere westerlies during the holocene. *Climate of the Past*
450 *Discussions* **7**(2), 339-347.
- 451 Wyrski, K, 1973: Teleconnections in the Equatorial Pacific Ocean. *Science* **180**,
452 66-68.
- 453 Wyrski, K, 1975: El Niño—the dynamic response of the equatorial Pacific Ocean to
454 atmospheric forcing. *J. Phys. Oceanogr.* **5**, 572-584.
- 455 Yu, Z., McCreary, J. P. J., Kessler, W. S. & Kelly, K. A, 2000: Influence of Equatorial
456 Dynamics on the Pacific North Equatorial Countercurrent. *J. Phys. Oceanography*.
457 **30**, 3179-3190.
- 458 Zou, Y.J, Xi, X.Y & Zhang, C.Y, 2017: Southward migrations of the Atlantic
459 Equatorial Currents during the Younger Dryas. *Limnology and Oceanography*. **62**,



460 1732-1741.